Interaction of Lipocalin 2, Transferrin, and Siderophores Determines the Replicative Niche of *Klebsiella pneumoniae* during Pneumonia

Michael A. Bachman,[a,b] Steven Lenio,[b] Lindsay Schmidt,[b] Jennifer E. Oyler,[c] and Jeffrey N. Weiser[c,d]

Department of Pathology, University of Pennsylvania School of Medicine, Philadelphia, Pennsylvania, USA[a]; Department of Pathology, University of Michigan, Ann Arbor, Michigan, USA[b]; and Departments of Microbiology[c] and Pediatrics,[d] University of Pennsylvania School of Medicine, Philadelphia, Pennsylvania, USA

ABSTRACT **Pathogenic bacteria require iron for replication within their host. *Klebsiella pneumoniae* and other Gram-negative pathogens produce the prototypical siderophore enterobactin (Ent) to scavenge iron *in vivo*. In response, mucosal surfaces secrete lipocalin 2 (Lcn2), an innate immune protein that binds Ent to disrupt bacterial iron acquisition and promote acute inflammation during colonization. A subset of *K. pneumoniae* isolates attempt to evade Lcn2 by producing glycosylated Ent (Gly-Ent, salmochelin) or the alternative siderophore yersiniabactin (Ybt). However, these siderophores are not functionally equivalent and differ in their abilities to promote growth in the upper respiratory tract, lungs, and serum. To understand how Lcn2 exploits functional differences between siderophores, isogenic mutants of an Ent$^+$ Gly-Ent$^+$ Ybt$^+$ *K. pneumoniae* strain were inoculated into *Lcn2*$^{+/+}$ and *Lcn2*$^{-/-}$ mice, and the pattern of pneumonia was examined. Lcn2 effectively protected against the *iroA ybtS* mutant (Ent$^+$ Gly-Ent$^-$ Ybt$^-$). *Lcn2*$^{+/+}$ mice had small foci of pneumonia, whereas *Lcn2*$^{-/-}$ mice had many bacteria in the perivascular space. The *entB* mutant (Ent$^-$ Ybt$^+$ Gly-Ent$^-$) caused moderate bronchopneumonia but did not invade the transferrin-containing perivascular space. Accordingly, transferrin blocked Ybt-dependent growth *in vitro*. The wild type and the *iroA* mutant, which both produce Ent and Ybt, had a mixed phenotype, causing a moderate bronchopneumonia in *Lcn2*$^{+/+}$ mice and perivascular overgrowth in *Lcn2*$^{-/-}$ mice. Together, these data indicate that Lcn2, in combination with transferrin, confines *K. pneumoniae* to the airways and prevents invasion into tissue containing the pulmonary vasculature.**

IMPORTANCE **Gram-negative bacteria are a common cause of severe hospital-acquired infections. To cause disease, they must obtain iron and secrete the small molecule enterobactin to do so. Animal models of pneumonia using *Klebsiella pneumoniae* indicate that enterobactin promotes severe disease. Accordingly, the host defense protein lipocalin 2 exploits this common target by binding enterobactin and disrupting its function. However, pathogenic bacteria often make additional siderophores that lipocalin 2 cannot bind, such as yersiniabactin, which could make this host defense ineffective. This work compares the pattern and severity of pneumonia caused by *K. pneumoniae* based on which siderophores it produces. The results indicate that enterobactin promotes growth around blood vessels that are rich in the iron-binding protein transferrin, but yersiniabactin does not. Together, transferrin and lipocalin 2 protect this space against all types of *K. pneumoniae* tested. Therefore, the ability to acquire iron determines where bacteria can grow in the lung.**

Received 7 September 2012 **Accepted** 1 November 2012 **Published** 20 November 2012

Citation Bachman MA, Lenio S, Schmidt L, Oyler JE, Weiser JN. 2012. Interaction of lipocalin 2, transferrin, and siderophores determines the replicative niche of *Klebsiella pneumoniae* during pneumonia. mBio 3(6):e00224-11. doi:10.1128/mBio.00224-11.

Editor Scott Hultgren, Washington University School of Medicine

Address correspondence to Michael A. Bachman, mikebach@med.umich.edu.

Iron is an essential nutrient required by humans and bacteria for fundamental processes including cellular respiration and DNA synthesis and incorporated into heme and iron-sulfur cluster containing proteins (1, 2). However, iron can be toxic by causing formation of hydroxyl radicals via the Fenton reaction. Under aerobic conditions, ferric [Fe(III)] iron is rendered insoluble through formation of oxyhydroxide polymers. To prevent these reactions, iron is generally complexed within enzymatic, carrier, and storage proteins in both humans and bacteria.

During an infection, invading bacteria must acquire iron for replication. In the mammalian host, this requires scavenging of iron from carrier proteins, such as transferrin in the blood, lactoferrin present along the mucosal surface, or heme from red blood cells (3). Some bacteria express surface receptors for these molecules and internalize them to access their iron. Others, including the *Enterobacteriaceae* family of Gram-negative bacteria, secrete iron-scavenging molecules called siderophores with extremely high affinities for iron. These siderophores can scavenge the trace amounts of free iron in the microenvironment or compete directly with mammalian carrier proteins for iron. The prototypical siderophore is enterobactin (Ent), which contains three catechol rings that coordinate a molecule of iron with the highest iron affinity of any known chelator (K_d of 10^{-35} M at physiological pH) (4). Pathogens may also produce siderophores in addition to Ent. Salmochelins are glycosylated forms of Ent (Gly-Ent), whose synthesis, export, and import proteins are encoded by the *iroA* locus (5). Yersiniabactin (Ybt) is a phenolate-type siderophore that is structurally distinct from Ent (6).

This diversity of siderophores suggests specialization of function. One potential function is to evade host defenses. Indeed, Ent-dependent iron acquisition is completely disrupted by the host protein lipocalin 2 (Lcn2). Lcn2 is a cup-shaped protein containing a ligand binding pocket with high affinity for Ent. By binding Ent, Lcn2 is bacteriostatic to isolates of *Escherichia coli* that depend on Ent-scavenged iron for growth in serum (7, 8). However, glycosylation of Ent is sufficient to prevent binding and support growth in serum and in a murine sepsis model (9). Another function of siderophores is tissue-specific iron acquisition. For example, *Yersinia pestis* Ybt is required to cause bubonic plague when inoculated subcutaneously but is dispensable in serum (10). However, these specialized siderophores may not be functionally equivalent to Ent. Yersiniabactin has a lower estimated affinity for iron than Ent (11). Gly-Ent is more hydrophilic than Ent and differs in its membrane partitioning and binding to serum albumin (5, 12, 13).

Klebsiella pneumoniae is a pathogenic member of the *Enterobacteriaceae* family and a leading cause of hospital-acquired pneumonia, sepsis, and urinary tract infections in the United States (14, 15). This pathogen is of increasing concern due to increasing carriage of a *K. pneumoniae* carbapenemase (KPC), rendering some isolates resistant to almost all available antibiotics (16). In addition to its polysaccharide capsule, *K. pneumoniae* siderophores are known virulence factors (15). In a prospective sampling of colonizing and invasive *K. pneumoniae* clinical isolates, 81% encoded Ent, 17% encoded Ent and Ybt, and 2% encoded combinations of Ent, Gly-Ent, and Ybt synthesis systems (17). Ent^+ Ybt^+ strains were significantly overrepresented among respiratory tract isolates and KPC-encoding strains.

In a murine model of bacterial pneumonia, the severity of disease varies greatly based on the interaction of bacterial siderophores and Lcn2 (17). Consistent with its bacteriostatic effects, mice producing Lcn2 that were infected with Ent^+ *K. pneumoniae* had a low lung bacterial burden, rare or no bacteria in the spleen, and no mortality. $Lcn2^{-/-}$ mice had a high lung bacterial burden (>1,000 fold increase), a high spleen burden, and high mortality (>60% at 3 days). Ybt promoted growth in the presence of Lcn2, since $Lcn2^{+/+}$ mice infected with an Ent^+ Ybt^+ or Ent^+ Ybt^+ Gly-Ent^+ strain had a moderate bacterial burden in the lungs and spleen but low mortality (<25%). However, neither strain promoted the severe disease caused by Ent^+ *K. pneumoniae* in the absence of Lcn2.

As shown for Ybt in *Y. pestis*, each siderophore may function only in a particular microenvironment. Therefore, differences in total bacterial burdens based on siderophore production may be due to global effects of Lcn2 or protection of certain sites within the lung. The lung is composed of distinct compartments, including the bronchial and bronchiolar airways, alveoli, interstitium, and vasculature. Infection of these sites by various bacterial and viral pathogens leads to disease patterns of bronchopneumonia, lobar pneumonia, or interstitial pneumonia that differ in severity. The host and bacterial factors that determine these patterns of pneumonia are not well understood. For *K. pneumoniae*, which causes bronchopneumonia and consolidation leading to severe lobar pneumonia (18, 19), siderophores may determine the replicative niche of the bacteria and therefore the pattern of disease. To test this hypothesis, the pattern of infection and localization of bacteria was compared between $Lcn2^{+/+}$ and $Lcn2^{-/-}$ mice infected with strains of *K. pneumoniae* producing combinations of Ent, Ybt, and Gly-Ent.

RESULTS

Enterobactin promotes replication in the perivascular space only in the absence of *Lcn2*. To examine directly the severity of pneumonia in $Lcn2^{+/+}$ and $Lcn2^{-/-}$ mice, infected lungs were examined microscopically. Phosphate-buffered saline (PBS)-mock-inoculated mice had normal lung architecture with little evidence of airway inflammation (Fig. 1A and 1B) regardless of the presence or absence of Lcn2. To determine the effect of bacterial siderophores on the pattern of pneumonia, isogenic mutants of an Ent^+ Gly-Ent^+ Ybt^+ *K. pneumoniae* strain (Table 1) were used to infect mice. To compare the severity and localization of infection, the involvement of the airways and perivascular spaces was scored in a blinded fashion. Three days after inoculation with the *iroA ybtS* mutant (Ent^+ Gly-Ent^- Ybt^-), $Lcn2^{+/+}$ mice had a mild total pathology score (Fig. 2A) (mean = 7.3) with slight airway localization (Fig. 2B) (mean = 1.3). The infection was characterized by localized areas of intense alveolar and bronchiolar inflammation consolidated into lobular/lobar pneumonia (Fig. 1A) and mild perivascular edema with some inflammatory cells (Fig. 1B). In $Lcn2^{-/-}$ mice, the total pathology score was greater (Fig. 2A) (mean = 13.3) and the localization switched from airway to perivascular involvement (Fig. 2B) (mean = −6.8, where a negative value denotes perivascular association). Although these mice had localized areas of alveolar and bronchiolar inflammation, there appeared to be enormous numbers of bacteria in the perivascular spaces intermixed with a moderate influx of inflammatory cells.

To confirm that these bacteria were *K. pneumoniae*, immunofluorescence analysis was performed. Staining of PBS mock-colonized mice demonstrated autofluorescent red blood cells in the vessel lumen but no staining in the perivascular space or lumen of the bronchioles (Fig. 3). Whereas the perivascular spaces of $Lcn2^{+/+}$ mice contained essentially no bacteria, $Lcn2^{-/-}$ mice had many intact rods that stained specifically with *K. pneumoniae* antiserum compared to results for the control lacking primary antibody. These data indicate that *K. pneumoniae* producing only Ent is able to replicate robustly in the perivascular space of $Lcn2^{-/-}$ mice.

Yersiniabactin supports bacterial replication in the airways regardless of *Lcn2*. *K. pneumoniae* producing only Ybt is able to replicate to moderate numbers in $Lcn2^{+/+}$ and $Lcn2^{-/-}$ mouse lungs (17, 20). To determine how Ybt influences bacterial pneumonia, an *entB* mutant (Ent^- Gly-Ent^- Ybt^+) was used to infect mice. In both $Lcn2^{+/+}$ and $Lcn2^{-/-}$ mice, the mice had a comparable, moderate pathology score (Fig. 2A) (mean = 11 and 9.3, respectively). Unlike the case of mice infected with the *iroA ybtS* mutant, there was little difference in the localization of infection between $Lcn2^{+/+}$ and $Lcn2^{-/-}$ mice (Fig. 2B) mean = 2 and −0.5, respectively). Both sets of mice had patchy, intense inflammation in the bronchioles and dense alveolar infiltrates, consistent with bronchopneumonia. There was also variable inflammation within the perivascular spaces (Fig. 1A and 1B). Based on immunofluorescence, there were many intact *K. pneumoniae* bacteria in the bronchioles and alveoli of both $Lcn2^{+/+}$ and $Lcn2^{-/-}$ mice (Fig. 3). However, there was no overgrowth of the *entB* mutant in the perivascular spaces of $Lcn2^{-/-}$ mice. These data indicate that Ybt is sufficient to promote robust replication in the airways re-

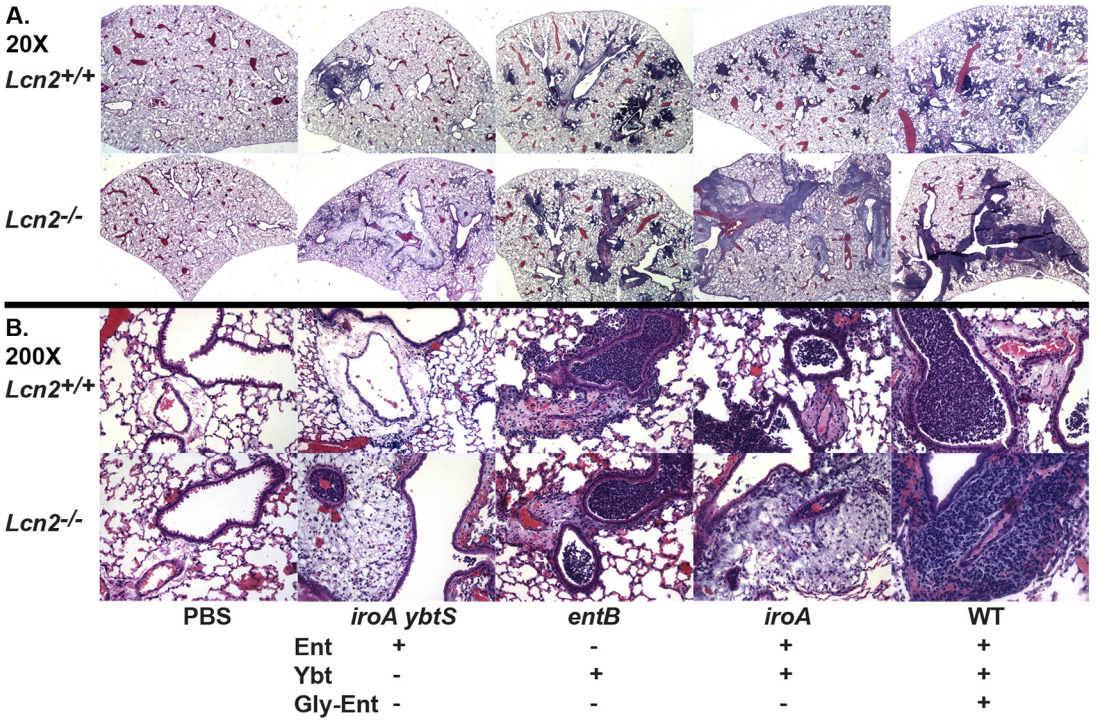

FIG 1 Lcn2-siderophore interactions determine the pattern of pneumonia caused by *K. pneumoniae*. Hematoxylin-and-eosin-stained formalin-fixed paraffin-embedded histological sections of lungs from $Lcn2^{+/+}$ and $Lcn2^{-/-}$ mice 3 days after retropharyngeal inoculation of 1×10^4 CFU/ml of wild-type (WT) or mutant *K. pneumoniae* producing the siderophores indicated (+) are shown at magnification 20× (A) or 200× (B).

gardless of Lcn2 but cannot support growth in the perivascular space.

Lcn2 prevents invasion of the perivascular space by *K. pneumoniae* producing multiple siderophores. *K. pneumoniae* bacteria producing both Ent and Ybt, including the epidemic KPC-producing sequence type 258, are overrepresented among respiratory isolates (17). To determine how the combination of these siderophores may influence the pattern of pneumonia, an *iroA* mutant (Ent^+ $Gly\text{-}Ent^-$ Ybt^+) was used to infect mice. $Lcn2^{+/+}$ mice had inflammation in both the bronchioles and alveoli (Fig. 1A and 1B), similar to the bronchopneumonia pattern caused by the *entB* mutant. These mice had a moderate pathology score (Fig. 2A) (mean = 13.8) and airway localization (Fig. 2B) (mean = 7.3). Based on immunofluorescence, there were many intact bacteria within the inflamed bronchi, bronchioles, and alveoli. Few bacteria were present in the perivascular spaces relative to adjacent inflamed airways. $Lcn2^{-/-}$ mice had a higher pathology score (Fig. 2A) (mean = 16.8) and a shift to perivascular localization (Fig. 2B) (mean = −8.2). There was bronchopneumonia with intact bacteria seen by immunofluorescence throughout the airways. In addition, many bacteria were observed in the perivascular spaces of the lungs. Together, these data indicate that a strain producing both Ybt and Ent can cause pneumonia in the presence of Lcn2. However, attributable to its ability to bind Ent, Lcn2 prevents Ent-dependent replication in the perivascular space.

Some isolates of *K. pneumoniae* also secrete Gly-Ent, which is not bound by Lcn2. To determine the contribution of Gly-Ent to the development of pneumonia, two additional isogenic strains were used to infect mice. A *ybtS* mutant (Ent^+ $Gly\text{-}Ent^+$ Ybt^-) had variable pathology scores in $Lcn2^{+/+}$ and $Lcn2^{-/-}$ mice (Fig. 2A) (means of 18 and 10, respectively). In $Lcn2^{+/+}$ mice, the infection was more localized to the airways (Fig. 2B) (mean = 1), whereas in $Lcn2^{-/-}$ mice, the infection was more localized to the perivascular spaces (mean = −4). The wild-type strain (Ent^+ $Gly\text{-}Ent^+$ Ybt^+) caused a moderate bronchopneumonia (Fig. 2A) (mean pathology score = 7) in $Lcn2^{+/+}$ mice with a slight airway predominance (Fig. 2B) (mean total score = 2). Consistent with

TABLE 1 *Klebsiella pneumoniae* strains used in this study

Strain	Description	Siderophore produced			Reference
		Ent	Ybt	Gly-Ent	
Wild type	KPPR1; Rif^r derivative of ATCC 43816 (serotype O1:K2)	+	+	+	29
entB mutant	VK087; KPPR1 *entB*	−	+	−	20
ybtS mutant	VK088; KPPR1 *ybtS*	+	−	+	20
entB ybtS mutant	VK089; KPPR1 *entB ybtS*	−	−	−	20
iroA ybtS mutant	KP20; VK088 *iroB*::*kan*	+	−	−	8
iroA mutant	KP25; KPPR1*iroB*::*kan*	+	+	−	8

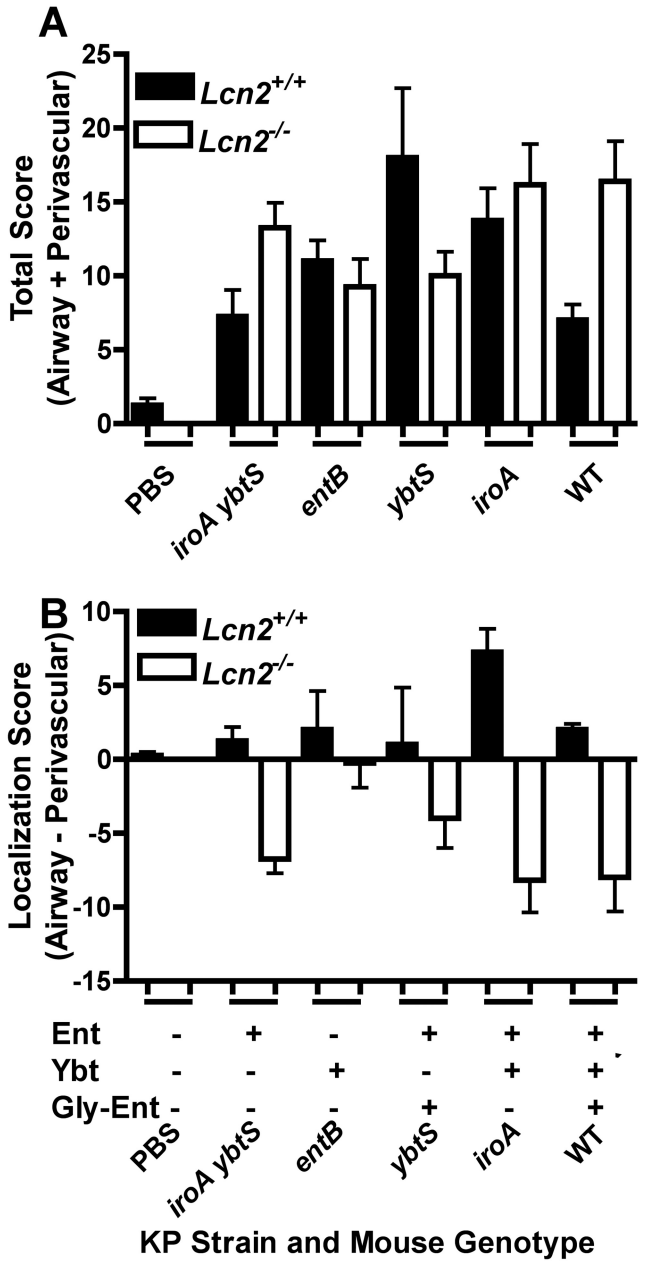

FIG 2 Severity and localization of lung pathology depends on the interaction of Lcn2 with enterobactin- and yersiniabactin-producing *K. pneumoniae*. Histological sections of lungs from $Lcn2^{+/+}$ and $Lcn2^{-/-}$ mice 3 days after retropharyngeal inoculation of 1×10^4 CFU/ml of *K. pneumoniae* were scored by a pathologist for severity and extent of involvement of the airways and perivascular spaces; $n \geq 4$ mice per group. The mean total (A) or localization (B) score is shown for each mouse genotype infected with wild-type (WT) or mutant *K. pneumoniae* producing the siderophores indicated (+). A positive localization score indicates airway predominance; a negative score indicates perivascular predominance.

the ability of Gly-Ent to promote growth in serum (8, 17), there were also perivascular infiltrates that contained *K. pneumoniae* (Fig. 3). However, in $Lcn2^{-/-}$ mice, there was more-severe infection (Fig. 2A) (mean pathology score = 16.4), with a marked increase in the amount of *K. pneumoniae* in the perivascular space (Fig. 1 and 2B) (mean localization score = −8). This correlates with the protection observed previously in $Lcn2^{+/+}$ mice infected with the wild type, as measured by lung and spleen CFU (17). Therefore, Lcn2 offers partial protection during pulmonary infection, even against *K. pneumoniae* making multiple siderophores.

The perivascular space contains serum exudate including transferrin. The observation that the *iroA ybtS* mutant can replicate in the perivascular space whereas the *entB* mutant cannot indicates nonredundant siderophore function. Increased vascular permeability is a defining component of acute inflammation, leading to leakage of protein-rich exudate from blood vessels (21). Therefore, the perivascular space likely contains blood components that inhibit growth of the *entB* mutant in serum (8). The iron carrier transferrin is present in large quantities and is the major source of iron in serum. To determine if the perivascular space contains transferrin as a marker of an inflammatory exudate, immunofluorescence analysis was performed (Fig. 4). Consistent with a well-controlled infection, $Lcn2^{+/+}$ mice infected with *iroA ybtS* mutant *K. pneumoniae* showed intravascular transferrin visualized as lacy fluorescence (Fig. 4A). However, in all other infections (Fig. 4A and 4B), transferrin was detected in the perivascular spaces. This is in contrast to the intraluminal staining of PBS-mock-colonized mice (Fig. 4D) and the autofluorescence of luminal red blood cells seen in the no-primary-antibody control (Fig. 4E). Consistent with the pattern seen by *Klebsiella*-specific immunofluorescence (Fig. 3), 4′,6-diamidino-2-phenylindole (DAPI)-stained bacteria were seen in transferrin-containing perivascular spaces of $Lcn2^{-/-}$ mice infected with *iroA* mutant or *iroA ybtS* mutant but not *entB* mutant *K. pneumoniae* (Fig. 4C). These data, combined with the patterns of infection described above, indicate that Ent-producing *K. pneumoniae* can replicate in serum-containing tissue, whereas the Ybt-dependent *entB* mutant cannot.

Serum transferrin inhibits Ybt-dependent growth. The mechanism by which serum inhibits growth of Ybt-dependent *K. pneumoniae* is unclear. To test the hypothesis that Ybt has lower growth-stimulatory activity in serum than Ent and Gly-Ent, equimolar amounts of siderophore were used to stimulate growth of an *entB ybtS* mutant (Ent^- Gly-Ent^- Ybt^-). Without addition of siderophores, this mutant was significantly defective in serum growth compared to the wild type (Fig. 5A). Addition of either Ent or Gly-Ent significantly stimulated growth in serum (Fig. 5B) at 0.1 μM, and both Ent and Gly-Ent restored growth to that of the wild type at 10 μM. In contrast, addition of Ybt stimulated growth only at 25 μM.

Next, the ability of serum to inhibit Ybt activity was tested under conditions of Ybt-dependent growth. LB medium treated with the iron chelator 2,2′-dipyridyl (DIP) was inoculated with *K. pneumoniae* mutants producing Ent (*iroA ybtS*), Ybt (*entB*), both (*iroA*), or neither siderophore (*entB ybtS*). The *iroA* and *iroA ybtS* mutants grew rapidly despite the addition of DIP. The *entB* mutant had significant growth compared to the *entB ybtS* mutant, attributable to endogenous production and utilization of Ybt (Fig. 6A). In contrast, all strains grew equivalently in LB alone (Fig. 6B). Addition of 1% serum had no significant effect on the *entB* mutant (Fig. 6C). However, addition of 10% serum significantly inhibited growth to levels comparable to that of the *entB ybtS* mutant (Fig. 6D). In contrast, *iroA* and *iroA ybtS* mutants grew robustly in both concentrations of serum.

To determine if transferrin is sufficient to reproduce the inhibitory effect of serum on the *entB* mutant, increasing amounts of

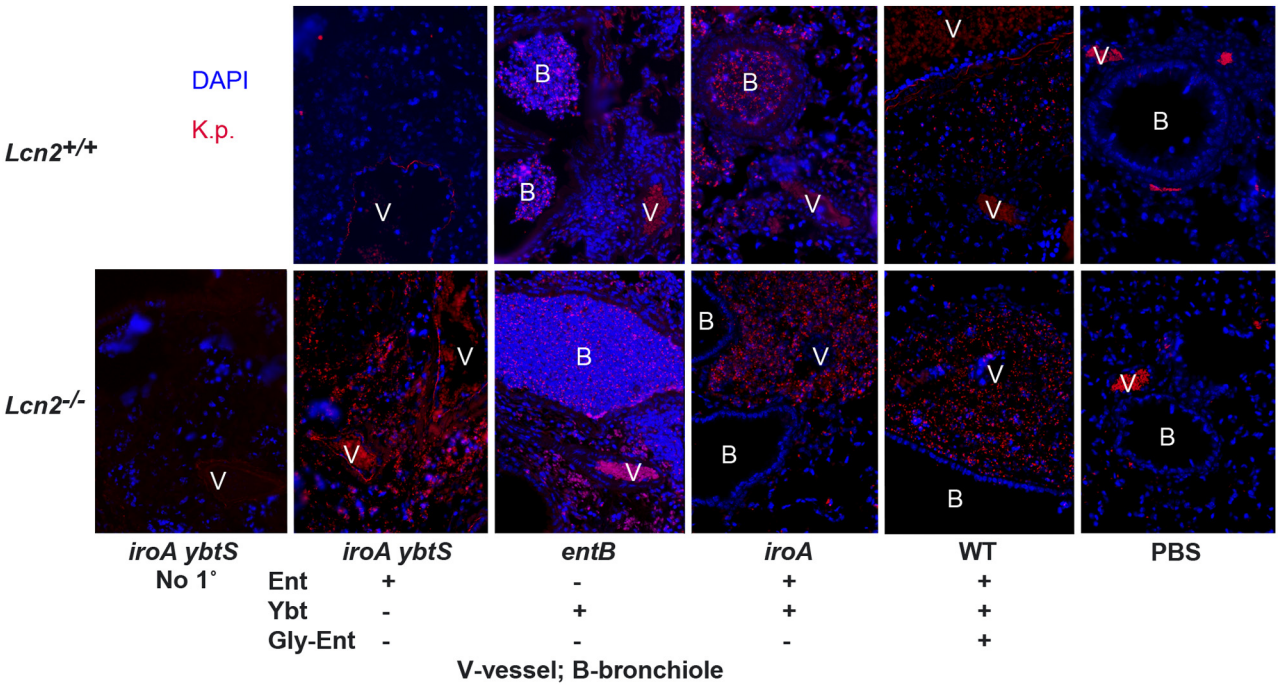

FIG 3 In the absence of Lcn2, enterobactin-producing *K. pneumoniae* infects the perivascular space, whereas a yersiniabactin-dependent mutant cannot. Images show immunofluorescence staining of formalin-fixed paraffin-embedded histological sections of lungs from $Lcn2^{+/+}$ and $Lcn2^{-/-}$ mice 3 days after retropharyngeal inoculation of 1×10^4 CFU/ml of WT or mutant *K. pneumoniae* encoding the siderophores indicated (+), using rabbit anti-*Klebsiella* serum and Cy3-conjugated goat anti-rabbit secondary antibody (red) and the nucleic acid stain DAPI (blue), except for "No 1°," in which anti-*Klebsiella* serum was omitted. Vessels (V) and bronchioles (B) are shown; magnification, ×200.

purified human transferrin were added (Fig. 6E and 6F). Transferrin added at 2.5 mg/ml, which is within the physiologic concentration range of human serum (2 to 4 mg/ml) (22), inhibited the *entB* mutant but not the *iroA* or *iroA ybtS* mutant. However, addition of Lcn2 significantly inhibited growth of both the *iroA* and *iroA ybtS* mutants (Fig. 6G). Therefore, the combination of Lcn2 and transferrin-containing exudate could protect the perivascular space from *K. pneumoniae* producing Ent and/or Ybt.

DISCUSSION

The pattern of pneumonia, as visualized by radiographic or histological analysis, correlates with the etiologic agent causing the disease. Bacterial infection may present as aspiration pneumonia, bronchopneumonia, or lobar pneumonia. In contrast, viral and mycoplasma infections typically demonstrate an interstitial pattern (21, 23). This study, comparing the pathology caused by *K. pneumoniae* bacteria producing various siderophores, indicates that the pattern of bacterial pneumonia is influenced by the ability of the pathogen to acquire iron. Ent^+ *K. pneumoniae* represents the most common phenotype in our collection of clinical isolates (17). Representing this phenotype, the *iroA ybtS* mutant causes limited, multifocal pneumonia consistent with inoculation by aspiration. Ent^+ Ybt^+ *K. pneumoniae* bacteria are a significant subset of clinical respiratory isolates, including KPC-producing strains. The Ent^+ Ybt^+ *iroA* mutant elicits an infiltrate of neutrophils in the bronchi, bronchioles, and adjacent airways, consistent with bronchopneumonia. Infection with this type of *K. pneumoniae* can also progress to larger areas of consolidation in the lung.

The difference in lung pathology between Ent^+ and Ent^+ Ybt^+ *K. pneumoniae* is dependent on the interaction of siderophores and Lcn2. Ent is counteracted by Lcn2, which effectively contains the infection to the site of inoculation. In contrast, Ybt is able to support replication in the presence of Lcn2, leading to greater lung pathology (Fig. 2) and greater density of bacteria in the lung (17). In the absence of Lcn2, both types of *K. pneumoniae* cause a severe pneumonia with a distinct pattern of inflammation and infection around blood vessels.

Recently, Ybt has been shown to bind copper in competition with iron during *E. coli* urinary tract infections and to prevent copper toxicity (24). Therefore, the effects of Ybt on *K. pneumoniae* growth may be attributable to copper binding, iron binding, or both. Preferential binding of Ybt to copper over iron may explain why exogenous Ybt can support growth of *K. pneumoniae* in serum but only at concentrations >100-fold higher than the effective dose of Ent or Gly-Ent. Similarly, Ybt may be unable to scavenge sufficient iron for growth in the presence of competing copper and transferrin, despite promoting growth on transferrin in isolation (11, 25). If the primary function of Ybt is to bind copper, then the inhibitory effect of serum and transferrin on the *entB* mutant may be due to inhibition of siderophore-independent iron acquisition rather than to Ybt itself. Because Ent can enhance copper toxicity (24), the *iroA ybtS* mutant may be more susceptible to copper toxicity than the *iroA* and *entB* mutants, contributing to its profound inhibition in $Lcn2^{+/+}$ mice. In turn, the moderate pneumonia caused by the *entB* mutant may be enabled by prevention of copper toxicity instead of enhanced iron acquisition. However, the *iroA* and *iroA ybtS* mutants both cause severe disease in $Lcn2^{-/-}$ mice, suggesting that the copper binding effect of Ybt is dispensable under certain conditions.

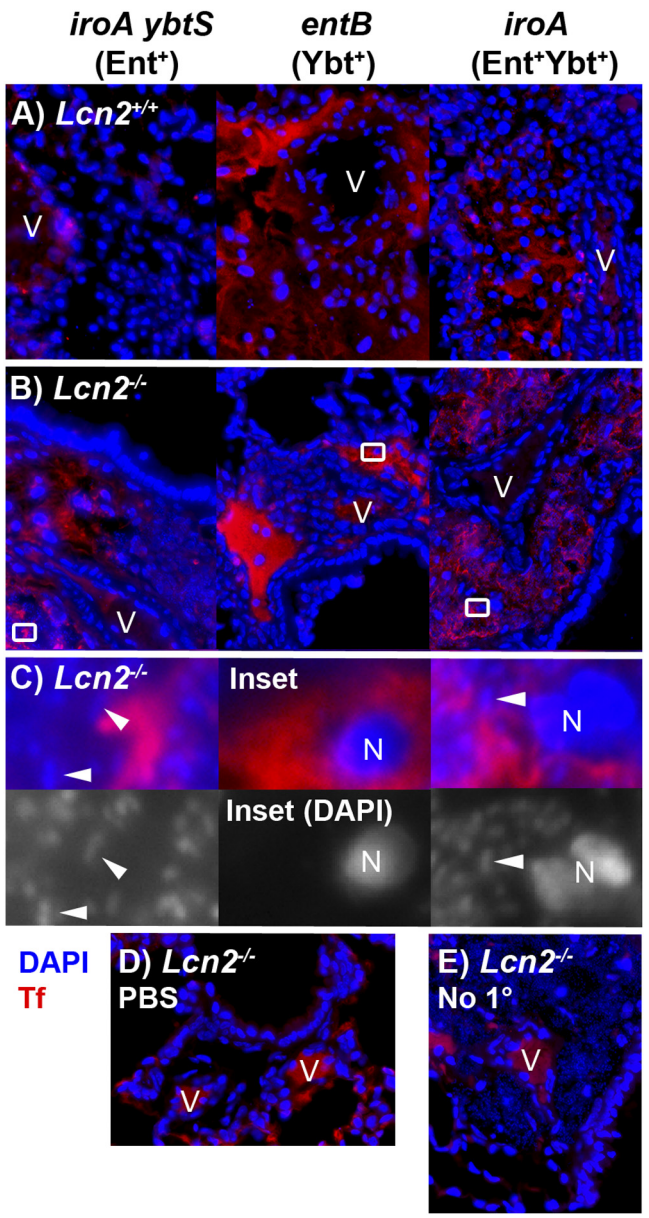

FIG 4 The perivascular spaces contain serum exudate as indicated by transferrin. Merged immunofluorescence images of formalin-fixed paraffin-embedded histological sections of lungs from $Lcn2^{+/+}$ (A) or $Lcn2^{-/-}$ (B) mice 3 days after retropharyngeal inoculation of 1×10^4 CFU/ml of *K. pneumoniae* siderophore mutants, stained using antitransferrin rabbit polyclonal IgG (Tf) (red) and the nucleic acid stain DAPI (blue), are shown. Magnified merged and DAPI-only images (C) of insets from $Lcn2^{-/-}$ mice in panel B demonstrate nuclei (N) and collections of bacteria (representative bacilli are indicated by arrowheads) in the perivascular space. Merged images of $Lcn2^{-/-}$ mice mock infected with PBS (D) or infected with *iroA* mutant *K. pneumoniae* but lacking antitransferrin antibody (E) are shown as controls. Magnification, ×400, except panel C (×4,000); V, vessels.

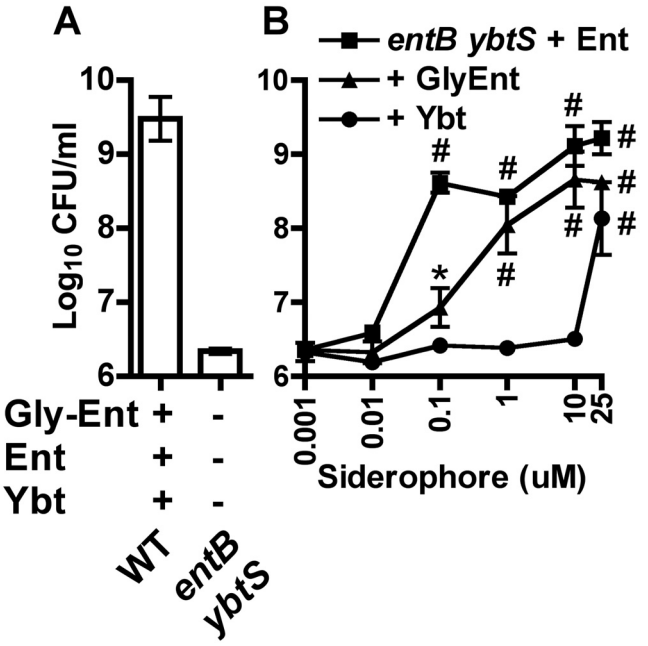

FIG 5 Ybt is less efficient than Ent and Gly-Ent at iron acquisition in serum. Bacterial densities after overnight growth in RPMI supplemented with 10% human serum of the wild type and *entB ybtS* mutant (A) or the *entB ybtS* mutant plus purified enterobactin (squares), glycosylated enterobactin (triangles), or yersiniabactin (circles) at the concentrations indicated (B) are shown. Means ± SEM from at least two independent experiments are shown. *, $P < 0.05$; #, $P < 0.01$, as measured by one-way analysis of variance (ANOVA) with Tukey's posttest compared to results for the *entB ybtS* mutant without added siderophore.

Ent and Ybt differ in their ability to support growth within niches of the lung. When unimpeded by Lcn2, Ent can support growth in the airways and perivascular spaces of the lung. In contrast, the *entB* mutant is confined to the airways and does not promote growth in the perivascular spaces. This defect is attributable to the inability of Ybt to promote growth in the presence of serum transferrin. In contrast, lactoferrin did not have a consistent effect on growth *in vitro* (data not shown).

The inability of Ybt to support growth in serum indicates that the iron chelating ability of inflammatory exudate compensates for gaps in Lcn2 siderophore specificity. In the presence of Lcn2, changes in vascular permeability may allow efflux of inflammatory cells without providing an accessible iron source for bacteria. Specifically, Lcn2 inhibits Ent and serum transferrin inhibits Ybt-dependent growth, either directly or indirectly. In the absence of Lcn2, all Ent-producing strains can invade the perivascular spaces. This leads to overwhelming bacterial growth in these spaces (Fig. 3) and corresponds with dissemination to the spleen and systemic illness (17).

The role of Gly-Ent (salmochelin) during *K. pneumoniae* lung infection remains unclear. In *E. coli*, production of Gly-Ent is sufficient to promote pulmonary infection in an avian air sac model (26). Accordingly, the ability of *K. pneumoniae* to produce Gly-Ent (*ybtS* mutant) compared to Ent alone (*iroA ybtS* mutant) correlates with worsened disease. Perhaps because only a portion of Ent is glycosylated (8, 17), the *ybtS* mutant caused infections with various overall severities (Fig. 2). In $Lcn2^{+/+}$ mice, the ability to produce Gly-Ent did not appear to worsen the infection compared to findings for mutants that produce Ybt. Despite their ability to grow in mouse serum containing Lcn2 (8), both Gly-Ent-producing strains primarily infected the airways of $Lcn2^{+/+}$ mice and switched to perivascular involvement in $Lcn2^{-/-}$ mice. Furthermore, Lcn2 significantly inhibited bacterial density of the wild type (Ent^+ Gly-Ent^+ Ybt^+) (17). Ent may be more efficient than

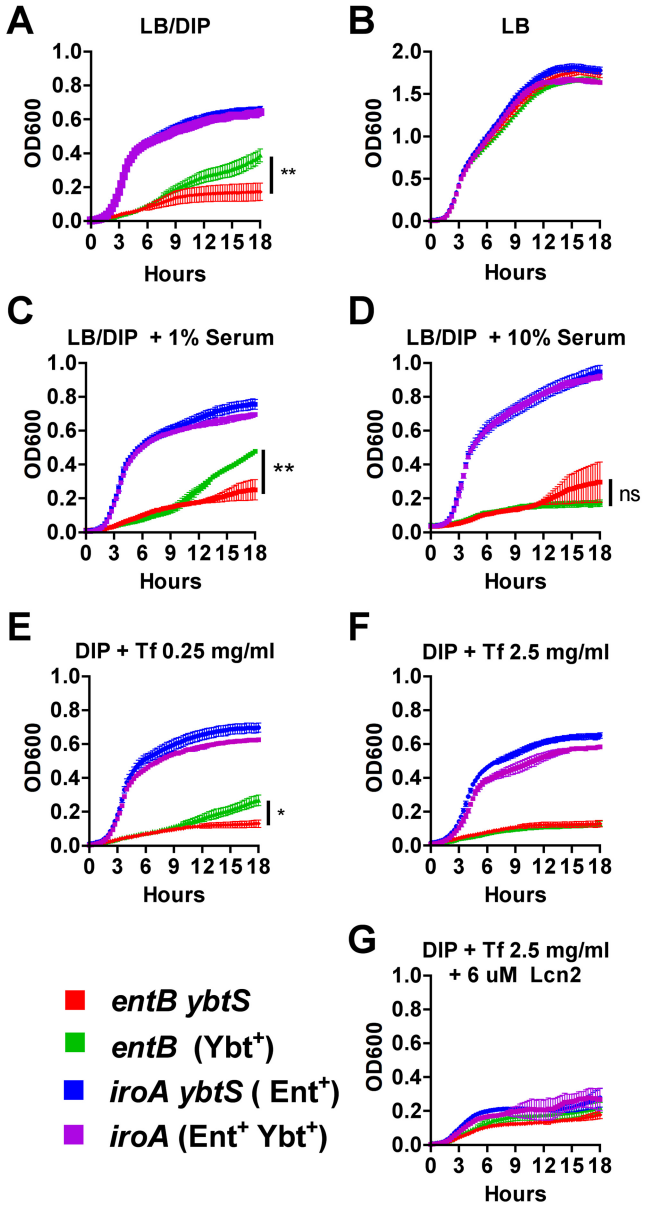

FIG 6 Serum or the serum component transferrin inhibits Ybt-dependent growth. *K. pneumoniae* growth was measured by optical density at 600 nm (OD_{600}) over 18 h in LB broth iron depleted with addition of 350 μM 2,2′-dipyridyl (DIP) (A), LB alone (B), LB-DIP with 1% (C) or 10% (D) pooled heat-inactivated human serum, LB-DIP with 0.25 (E) or 2.5 mg/ml (F) purified human transferrin, or 2.5 mg/ml transferrin plus 6 μM recombinant human Lcn2 (G) during incubation at 37°C with intermittent agitation. Means ± SEM are shown for three replicates and are representative of two independent experiments. Final OD_{600}s between strains were compared using one-way ANOVA with Tukey's multiple-comparison test (*, $P < 0.05$; **, $P < 0.01$; ns, not significant).

Gly-Ent at acquiring iron in the perivascular spaces, or the ability of Lcn2 to sequester Ent as a significant proportion of the total siderophore pool may account for its partial protection against the wild type that produces three siderophores.

In summary, this work demonstrates that the interaction between Lcn2, transferrin, and bacterial siderophores determines the replicative niche of *K. pneumoniae* in the lung. Transferrin is an efficient barrier against Ybt-dependent bacterial growth. Lcn2 is sufficient to inhibit the progression of pneumonia caused by *K. pneumoniae* producing only Ent, comprising the majority of isolates. Importantly, Lcn2 protects the perivascular space from a virulent subset of strains that produce multiple siderophores. Defense of the perivascular space is crucial, since invasion leads to intense bacterial growth, systemic spread, and potentially fatal disease.

MATERIALS AND METHODS

Bacterial strains and media. All *K. pneumoniae* strains used are rifampin-resistant derivatives of ATCC 43816, and their construction has been described previously (Table 1). *K. pneumoniae* was cultured in Luria-Bertani broth with agitation at 37°C or agar at 30°C overnight, supplemented with rifampin (30 μg/ml; all strains) and kanamycin (50 μg/ml; KP20 and KP25).

Murine pneumonia model. All animal studies were approved by the University of Pennsylvania Institutional Animal Care and Use Committee. *Lcn2*$^{-/-}$ mice (7) that had been backcrossed with C57BL/6 mice or their wild-type counterparts (*Lcn2*$^{+/+}$) were used. Infections were carried out as previously described (17). Briefly, overnight cultures of *K. pneumoniae* were collected by centrifugation and diluted in phosphate-buffered saline, and 1×10^4 CFU was administered in 50 μl of saline into the pharynx of mice under isoflurane anesthesia. Three days after infection, mice were sacrificed by CO_2 asphyxiation. For histological examination, lungs were perfused with 10% normal buffered formalin (Sigma) via tracheal instillation and ligation, paraffin embedded, sectioned, and stained with hematoxylin and eosin (H&E).

Scoring of lung pathology. Histological sections were scored by a pulmonary pathologist in a blinded fashion, using a modified version of the system of Stapleton et al. (27). An airway severity score was assigned as follows: 0, no involvement; 1, localized infiltrates of neutrophils within the alveolar sacs with increased alveolar macrophages, no bacteria seen; 2, dense infiltrates of neutrophils in bronchioles and larger airways with involvement of adjacent alveoli, no bacteria seen; 3, consolidation of neutrophil inflammation in bronchioles and adjacent alveoli, lobular or lobar pneumonia, or intact visible bacteria seen at magnification ×40 but inflammatory cells greater than bacteria; 4, overwhelming infection with bacteria greater than inflammatory cells in alveoli or bronchioles. A perivascular severity score was assigned as follows: 0, no involvement; 1, mild perivascular infiltrates without involvement of the peribronchiolar regions, no bacteria seen; 2, moderate perivascular and peribronchiolar infiltrates, no bacteria seen; 3, severe perivascular and peribronchiolar infiltrates or intact visible bacteria seen at magnification ×40 but inflammatory cells greater than bacteria; 4, overwhelming infection with bacteria greater than inflammatory cells in perivascular and peribronchiolar regions. A modifier score for severity was determined for both airway and perivascular sites on the following scale: 0, no inflammation or infection seen;1, 1 to 10% involvement by either inflammatory cells or intact bacteria; 2, 11 to 20% involvement by either inflammatory cells or intact bacteria; 3, 21 to 30% involvement by either inflammatory cells or intact bacteria; 4, >30 percentage point involvement by either inflammatory cells or intact bacteria. For each mouse, a total score was calculated as (airway score × airway modifier) + (perivascular score × perivascular modifier) and a localization score was calculated as (airway score × airway modifier) − (perivascular score × perivascular modifier).

Immunofluorescence microscopy. Slides with paraffin sections were warmed to 60°C, and paraffin was removed by stepwise treatment with xylene (twice, 4 min each), 100% ethanol (twice, 2 min each), and 1 min each of 95%, 90%, 80%, and 70% ethanol. Slides were then rinsed in water. For *Klebsiella* immunofluorescence, antigen retrieval was performed in Tris-EDTA buffer (Tris base, 1.2 g/liter; EDTA, 0.37 g/liter), pH 8, by microwaving for 15 min and cooling for 15 min (28). Slides were washed in saline and treated with starting block reagent for 10 min. The primary antibody was diluted in saline containing 0.1% bovine serum

albumin and 0.2% Triton X-100 and incubated on the slides overnight at 4°C. Rabbit anti-*Klebsiella* serum (United States Biologicals) was used at 1:4,000; rabbit anti-mouse transferrin (R&D Systems) was used at 1:50. Slides were washed in PBS and stained with Cy3-conjugated donkey anti-rabbit antibody diluted 1:600 in PBS with albumin and Triton X-100 for 30 min at 37°C. Slides were washed, stained with a 1:10,000 dilution of DAPI in water for 20 s, and washed in water, and coverslips were mounted with Kirkegaard & Perry mounting medium.

***In vitro* growth assays.** Iron-limited medium was prepared by supplementing Luria-Bertani broth with the iron chelator 2,2′-dipyridyl (Acros) to a final concentration of 350 μM. Where indicated, increasing concentrations of human serum, partially saturated human transferrin (Sigma), and recombinant human Lcn2 were added. Purification of Lcn2 was performed as previously described (17). Overnight cultures of *K. pneumoniae* were diluted 1:10,000 in saline, and 10 μl was added to 100 μl of iron-limited broth with or without supplements. Samples were incubated overnight in 96-well plates at 37°C. To assay the effect of exogenous siderophores, dilutions of *K. pneumoniae* were prepared and incubated as above in RPMI medium (Invitrogen) containing 10% human serum and increasing concentrations of the purified siderophores enterobactin, yersiniabactin, and salmochelin S4 (EMC microcollections). To measure bacterial density, samples were serially diluted in saline and plated on agar with appropriate antibiotics.

ACKNOWLEDGMENTS

This work was supported by Public Health Service grant GM085612 from the National Institute of General Medical Sciences. H&E and immunofluorescence staining was facilitated by the Morphology Core of the Center for the Molecular Studies of Liver and Digestive Disease at the University of Pennsylvania (center grant P30 DK50306).

M.A.B. thanks Harry Mobley for critical review of the manuscript, Leslie Litzky for discussing pathological diagnoses, and Jason Weinberg for guidance about histology scoring.

REFERENCES

1. **Earhart CF.** 1996. Uptake and metabolism of iron and molybdenum. *In* Neidhart F (ed), *E. coli* and *salmonella*. ASM Press, Washington, DC.
2. **Nairz M, Schroll A, Sonnweber T, Weiss G.** 2010. The struggle for iron—a metal at the host-pathogen interface. Cell. Microbiol. **12**: 1691–1702.
3. **Skaar EP.** 2010. The battle for iron between bacterial pathogens and their vertebrate hosts. PLoS Pathog. **6**:e1000949. http://dx.doi.org/doi:10.1371/journal.ppat.1000949.
4. **Lin H, Fischbach MA, Liu DR, Walsh CT.** 2005. *In vitro* characterization of salmochelin and enterobactin trilactone hydrolases IroD, IroE, and Fes. J. Am. Chem. Soc. **127**:11075–11084.
5. **Hantke K, Nicholson G, Rabsch W, Winkelmann G.** 2003. Salmochelins, siderophores of *Salmonella enterica* and uropathogenic *Escherichia coli* strains, are recognized by the outer membrane receptor IroN. Proc. Natl. Acad. Sci. U. S. A. **100**:3677–3682.
6. **Miethke M, Marahiel MA.** 2007. Siderophore-based iron acquisition and pathogen control. Microbiol. Mol. Biol. Rev. **71**:413–451.
7. **Flo TH, et al.** 2004. Lipocalin 2 mediates an innate immune response to bacterial infection by sequestrating iron. Nature **432**:917–921.
8. **Bachman MA, Miller VL, Weiser JN.** 2009. Mucosal lipocalin 2 has pro-inflammatory and iron-sequestering effects in response to bacterial enterobactin. PLoS Pathog. **5**:e1000622.
9. **Fischbach MA, et al.** 2006. The pathogen-associated *iroA* gene cluster mediates bacterial evasion of lipocalin 2. Proc. Natl. Acad. Sci. U. S. A. **103**:16502–16507.
10. **Bearden SW, Perry RD.** 1999. The Yfe system of *Yersinia pestis* transports iron and manganese and is required for full virulence of plague. Mol. Microbiol. **32**:403–414.
11. **Perry RD, Balbo PB, Jones HA, Fetherston JD, DeMoll E.** 1999. Yersiniabactin from *Yersinia pestis*: biochemical characterization of the siderophore and its role in iron transport and regulation. Microbiology **145**(Pt 5):1181–1190.
12. **Bister B, et al.** 2004. The structure of salmochelins: C-glucosylated enterobactins of *Salmonella enterica*. Biometals **17**:471–481.
13. **Luo M, et al.** 2006. Enzymatic tailoring of enterobactin alters membrane partitioning and iron acquisition. ACS Chem. Biol. **1**:29–32.
14. **Jones RN.** 2010. Microbial etiologies of hospital-acquired bacterial pneumonia and ventilator-associated bacterial pneumonia. Clin. Infect. Dis. **51**(Suppl 1):S81–S87.
15. **Podschun R, Ullmann U.** 1998. *Klebsiella* spp. as nosocomial pathogens: epidemiology, taxonomy, typing methods, and pathogenicity factors. Clin. Microbiol. Rev. **11**:589–603.
16. **Kitchel B, et al.** 2009. Molecular epidemiology of KPC-producing *Klebsiella pneumoniae* isolates in the United States: clonal expansion of multilocus sequence type 258. Antimicrob. Agents Chemother. **53**:3365–3370.
17. **Bachman MA, et al.** 2011. *Klebsiella pneumoniae* yersiniabactin promotes respiratory tract infection through evasion of lipocalin 2. Infect. Immun. **79**:3309–3316.
18. **Okada F, et al.** 2009. Clinical and pulmonary thin-section CT findings in acute *Klebsiella pneumoniae* pneumonia. Eur. Radiol. **19**:809–815.
19. **Franquet T.** 2001. Imaging of pneumonia: trends and algorithms. Eur. Respir. J. **18**:196–208.
20. **Lawlor MS, O'Connor C, Miller VL.** 2007. Yersiniabactin is a virulence factor for *Klebsiella pneumoniae* during pulmonary infection. Infect. Immun. **75**:1463–1472.
21. Kumar V, Abbas AK, Fausto N (eds.). 2005. Robbins pathologic basis of disease, 7th ed. Elsevier Saunders, Philadelphia, PA.
22. **McPherson RA.** 2007. Specific proteins, p 238. *In* McPherson RA, Pincus MR (ed), Henry's clinical diagnosis and management by laboratory methods. Saunders Elsevier, Philadelphia, PA.
23. **Goodman LR.** 1999. Felson's principles of chest roentgenology. W.B. Saunders, Philadelphia, PA.
24. **Chaturvedi KS, Hung CS, Crowley JR, Stapleton AE, Henderson JP.** 2012. The siderophore yersiniabactin binds copper to protect pathogens during infection. Nat. Chem. Biol. **8**:731–736.
25. **Aisen P, Leibman A, Zweier J.** 1978. Stoichiometric and site characteristics of the binding of iron to human transferrin. J. Biol. Chem. **253**: 1930–1937.
26. **Caza M, Lépine F, Milot S, Dozois CM.** 2008. Specific roles of the *iroBCDEN* genes in virulence of an avian pathogenic *Escherichia coli* O78 strain and in production of salmochelins. Infect. Immun. **76**:3539–3549.
27. **Stapleton CM, et al.** 2005. Enhanced susceptibility of staggerer (RORalpha$^{sg/sg}$) mice to lipopolysaccharide-induced lung inflammation. Am. J. Physiol. Lung Cell. Mol. Physiol. **289**:L144–L152.
28. **Twenhafel NA, et al.** 2008. Multisystemic abscesses in African green monkeys (*Chlorocebus aethiops*) with invasive *Klebsiella pneumoniae*—identification of the hypermucoviscosity phenotype. Vet. Pathol. **45**: 226–231.
29. **Lawlor MS, Hsu J, Rick PD, Miller VL.** 2005. Identification of *Klebsiella pneumoniae* virulence determinants using an intranasal infection model. Mol. Microbiol. **58**:1054–1073.